The failure probability of welded steel pipelines in dolomitic areas

D T Nel, J Haarhoff

This paper considers aspects related to the nature of dolomite, sinkholes, the risk classification of dolomitic land, as well as factors affecting the failure of pipelines in dolomitic areas. The information and data presented are used to derive equations that may be used to predict the probability of failure of steel pipelines in dolomitic areas subject to sinkhole formation. Consideration is also given to other factors that may influence the failure of pipelines in dolomitic areas.

TECHNICAL PAPER

JOURNAL OF THE SOUTH AFRICAN INSTITUTION OF CIVIL ENGINEERING

Vol 53 No 1, April 2011, Pages 9–21, Paper 751

DANIE NEL obtained his bachelor and master's degrees in civil engineering at the then Rand Afrikaans University and his D Ing degree at the University of Johannesburg. He spent his career in the municipal and bulk water supply environment and is currently an independent consultant. He has vast experience in many of the disciplines related to the provision, operation and maintenance of civil engineering infrastructure, bulk water supply infrastructure projects, risk assessment related to bulk water distribution, management, pipeline risk assessment in dolomitic areas, as well as bulk sanitation services.

Contact details:
PO Box 112
Meyerton
1961
South Africa
T: +27 (0)16 362 0772
F: +27 (0)86 550 3544
E: daclc@absamail.co.za

JOHANNES HAARHOFF graduated as civil and environmental engineer at the University of Stellenbosch and Iowa State University. Prof Haarhoff spent the first part of his career in municipal employ, civil construction, design and project management before joining the University of Johannesburg in 1990, where he leads the Water Research Group. This group focuses on both applied and fundamental aspects of drinking water treatment and supply.

Contact details:
PO Box 524
Auckland Park
2006
South Africa
T: +27 (0)11 559 2148
F: +27 (0)11 559 2395
E: jhaarhoff@uj.ac.za

INTRODUCTION

Sections of water distribution pipelines are often installed in dolomitic areas subject to sinkhole formation. The possibility of losing a bulk water pipeline through sinkhole formation, however remote, has an obvious and large impact on the reliability of water supply. This paper develops a methodology to estimate the failure probability of steel pipelines associated with sinkhole formation.

The assessment of the probability of sinkhole formation, and the related sinkhole diameter, draws on the substantial body of experience accumulated in South Africa in the past years. The data and guidelines had to be adapted for the purposes of this analysis. This had to be complemented with a structural and spatial analysis of a steel pipe intersecting a sinkhole. The workability of the approach is demonstrated with a hypothetical example. The paper closes with a critical assessment of the methodology and how it could be improved and refined.

THE NATURE OF DOLOMITE

Dolomitic land refers to areas underlain directly or at shallow depth by dolomite, which is a sedimentary rock, has a calcareous composition, is chemically formed and consists of the double carbonate of calcium and magnesium (Lurie 1977).

Chemical composition of dolomite:

$$3CaCO_3 2MgCO_3 \quad (1)$$

Dolomitic rock has a number of unique features (Brink 1979):

- It is a compact, impervious rock with a porosity of approximately 0,3%.
- It has a highly developed network of joints, tension-fractures and faults that allows water to percolate easily through the rock mass.
- It is easily dissolved by carbon dioxide in the groundwater. The carbon dioxide in conjunction with groundwater forms a weak carbonic acid, which dissolves the dolomite to bicarbonates.

$$\underset{\text{(Dolomite)}}{3CaCO_3 2MgCO_3} + \underset{\text{(Carbonic acid)}}{5H_2O_3}$$
$$= \underset{\text{(Calcium bicarbonate)}}{3Ca(HCO_3)_2} + \underset{\text{(Magnesium bicarbonate)}}{2Mg(HCO_3)_2} \quad (2)$$

- The main insoluble residues left from the weathering of dolomite are chert (SiO_2), iron from the layers of ferruginous dolomite, and wad.
- In the presence of a small concentration of manganese, the dolomite is found in the form of wad. Wad (or manganiferous earth) is an insoluble and highly compressible material that consists of manganese and iron oxides with minor impurities. A lowering of the water table may produce significant ground movement at the surface due to compression of the wad. This ground movement manifests itself as a doline, being a shallow enclosed depression in the ground surface. A doline can be from a few metres across to more than 1 km in length.

SINKHOLES

Types of sinkholes

Sinkholes (also referred to as sinks) are a type of land subsidence since they involve a vertical downward movement of the land surface. Three different types of sinkholes are distinguished (Tharp 1999; Waltham *et al* 2005):

Solution sinkholes (Figure 1) form where dolomitic bedrock is exposed at the land surface and subjected to weathering by dissolution. Surface water collects in natural depressions and the bedrock slowly dissolves to form a sinkhole.

Key words: dolomitic, sinkholes, pipeline, failure, probability

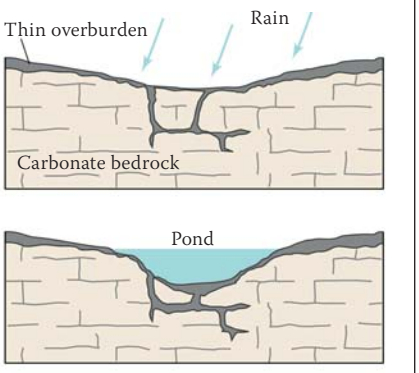

Figure 1 Solution sinkholes (www.sinkhole.org)

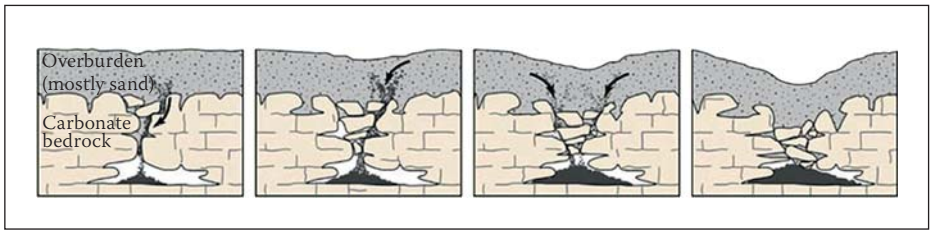

Figure 2 Cover subsidence sinkholes (www.sinkhole.org)

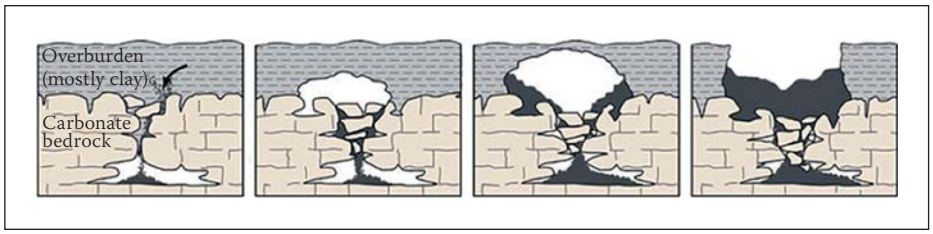

Figure 3 Cover collapse sinkholes (www.sinkhole.org)

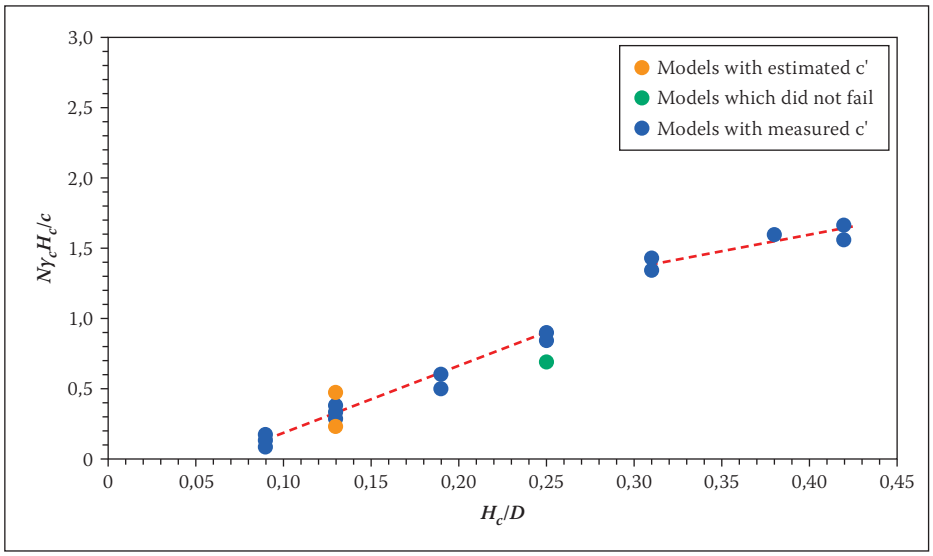

Figure 4 Sinkhole stability chart – cemented overburden (after Gooding *et al* 2002)

Cover subsidence sinkholes (Figure 2) are similar to solution sinkholes except that the soluble bedrock is covered by a thin layer of soil or sediment. Surface water infiltration dissolves the dolomite to form cavities where the bedrock is most intensely fractured, and the overlying sediment gradually moves downward into the expanding cavity.

Cover collapse sinkholes (Figure 3) form when surface materials suddenly drop into a subsurface cavity. A cavity will form slowly over time as groundwater moves along fractures in soluble bedrock and enlarges the cavity through dissolution. The actual collapse can occur in two different ways. Firstly, when a cavity gets sufficiently large, the roof of the cavity becomes too thin to support the weight of the overlying rock, sediment or imposed loads, so it collapses into the cavity. Secondly, caves filled with groundwater are sometimes able to support the weight of overlying sediment, but if groundwater levels are lowered, the overlying sediment will first erode and then collapse into the dewatered cavity. The final breakthrough of a cover collapse sinkhole can occur suddenly and it may have catastrophic consequences.

Sinkhole formation

Sinkholes result from the hollowing out or formation of a void below the earth's surface. Sinkholes can form naturally as a consequence of normal geological processes, or they may have anthropogenic causes. According to Schőning (1990) anthropogenic sinkhole formation requires three conditions – the right geotechnical conditions, inappropriate development relative to the geotechnical conditions and adequate rainfall. Anthropogenic causes such as the construction of roads, forming of drainage ditches, township development and the associated services, groundwater extraction, groundwater recharge, etc, may cause sinkholes to form.

Buttrick (1992) discussed various factors that may influence sinkhole formation and the size of the sinkhole that will form, namely:

- The receptacle within the bedrock or overburden that can receive the mobilised sinkhole material.
- The throat size of the conduit that feeds the mobilised soil material into the receptacle.
- The blanketing layer of material that overlies the dolomite bedrock.
- A mobilising agency that will induce mobilisation of the material in the blanketing layer through the throat and into the receptacle.
- The soil angle of internal friction.
- The presence and influence of intrusive layers within the blanketing layer that will reduce the mobilisation potential of materials in the blanketing layers.
- The position of the water table.

To gain a better understanding of the mechanisms of sinkhole formation, Goodings *et al* (2002) constructed and tested forty-nine physical models of sinkhole development in a laboratory. The models simulated weakly cemented sand overlying cavities in karst limestone, but did not consider the influence of groundwater. The models were divided into two groups – those with nothing above the weakly cemented sand layer, and those with an additional layer of loose, uncemented soil above the cemented sand layer. For the experiments with no uncemented soil overburden, the main findings were:

- The parameters critical to predicting failure were the unit weight of the cemented sand (g_c), the thickness of the cemented sand overlying the karst cavity (H_c), the true cohesion of the cemented sand (c') and the diameter of the underlying karst cavity (D).
- Failure was manifested as an intact plug of soil falling into the cavity below. Three modes of failure were observed:
  - In models with thin layers ($H_c/D <$ 0,25) failure occurred as a breakthrough plug that left a hole in the top of the weakly cemented layer but with little overhang on the inclines.
  - In models with H_c/D = 0,25, failure occurred as a breakthrough plug, but there was some overhang observed on the inclines.
  - In models with thick layers ($H_c/D \geq$ 0,31) failure occurred when a plug of

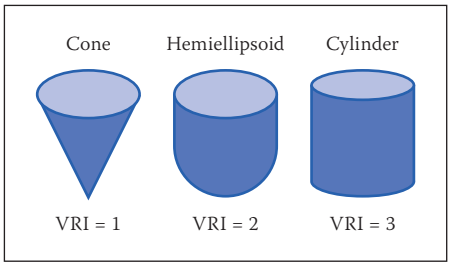

Figure 5 Geometry forms associated with whole number VRI values (after Hyatt *et al* 1996)

soil dropped into the underlying cavity, but the hole did not break through to the top of the weakly cemented soil layer.

A sinkhole stability chart was developed that can be used to predict full-scale failures under certain conditions, as shown in Figure 4. The x-axis value relates to the ratio of the depth of overburden and the diameter of the underlying cavity, whereas the y-axis value deals with the characteristics of the soil above the cavity where a sinkhole may possibly form. N is a scale factor with N = 1 for full scale models. The stability chart is for failure conditions and includes no factors of safety. If the plotted value of a specific scenario being investigated falls on or above the failure envelope, failure is predicted.

For the experiments with an uncemented soil overburden above the weakly cemented sand, the H_c/D ratio was kept at or below 0,25. The main finding was that the additional pressure of the uncemented soil bearing down on the breakthrough plug never exceeded the weight of a cone of sand of diameter D' and height 1,25D', where D' is the diameter of the top of the inclined breakthrough plug.

Sinkhole geometry

Three distinct forms related to sinkholes have been recognised, namely shaft, undercut and bowl forms (Hyatt *et al* 1996):

- Shaft forms are steep-sided, with a flat bottom.
- Undercut forms have a distinct overhang on at least three of the four sides.
- Bowl forms are simple depressions with side slopes less than or equal to 90 degrees.

Hyatt *et al* (1996) developed a three-dimensional volume ratio index (*VRI*) which compares the actual volume of the sinkhole (V_s) to the volume of an elliptical cone (V_{ec}) having the same major radii, minor radii and depth as the sinkhole that has formed, as defined by Equation 3.

$$VRI = \frac{V_s}{V_{ec}} = \frac{V_s}{\frac{1}{3} * \pi abd} \quad (3)$$

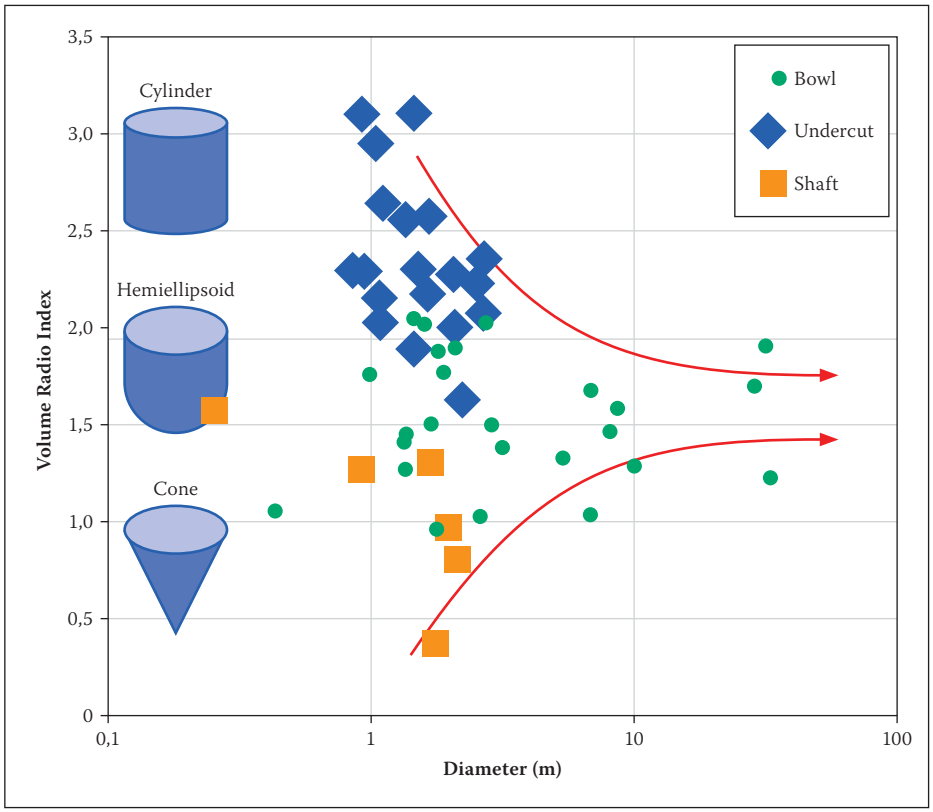

Figure 6 Comparison of sinkhole VRI values with average diameter of sinkhole in Georgia, USA (after Hyatt *et al* 1996)

where

VRI is the volume ratio index
V_s is the volume of the sinkhole that formed
V_{ec} is the volume of an elliptical cone with the same major radii, minor radii and depth as the sinkhole that formed
a is the major radii of the sinkhole that has formed (length / 2)
b is the minor radii of the sinkhole that has formed (width / 2)
d is the depth of the sinkhole that has formed

The *VRI* provides an indication of the geometric form to which the sinkhole is volumetrically most similar, as shown in Figure 5.

Figure 6 reflects the results of a study related to sinkholes that formed in the Dougherty Plain at Albany, Georgia in the USA (Hyatt *et al* 1996). For every sinkhole, the sinkhole *VRI* value was plotted against the diameter of the sinkhole. The results indicated that the generic form of small sinkholes (less than 2 m in diameter) varied greatly. As the sinkhole diameter increased, the *VRI* values converged to an ideal bowl form.

The parameter used to describe the surface shape of sinkholes is the ratio of the minor to the major surface dimension of the sinkhole. Sinkholes tend to show a circular or sub-elliptical shape, and the following ratios have been reported:

- Bruno *et al* (2008); predominantly in the range 0,62 to 1,0.
- Hyatt *et al* (1996); predominantly from 0,9 to 1,0, but sinkholes with ratios from 0,48 to 0,9 were also encountered.
- Brinkmann *et al* (2008); within a range of 0,153 to 0,954, with an average ratio of 0,715.

Pilecki *et al* (2006) presented the relationship given by Equation 4, which suggests that the greater the thickness of the layer of loose overburden, the greater the area of the sinkhole at the ground surface. Above a critical overburden thickness, however, the relationship breaks down and the sinkhole diameter remains constant, due to the so-called chimney action process.

$$D_{sh} = 2Z \tan(90 - \theta) + 2r_s \quad (4)$$

where

D_{sh} is the diameter of the sinkhole on the ground surface in m
Z is the thickness of the loose overburden in m
θ is the angle of internal friction of the loose overburden
r_s is the radius of the shaft that can receive the sinkhole material

Aspects pertaining to sinkholes are widely reported in the literature, but data related to the sizes of sinkholes that occurred is limited. Table 1 provides a summary of the dimensions of sinkholes as reflected in a

Table 1 Sinkhole dimensions – various sources

Area	Sinkhole type / form	Number of sinkholes	Mean diameter or length (m)	Maximum diameter or length (m)	Mean depth (m)	Maximum depth (m)
Galve *et al* (2009)						
Ebro Valley (Spain)	Cover collapse	447	2,5	20	0,7	8,0
	Cover collapse	39	5,9	15	2,3	15,5
	Cover and bedrock collapse	23	10,0	50	1,5	6,0
	Cover and bedrock collapse	91	43,3	114	3,0	6,8
	Cover and bedrock sagging	24	136,0*	850*	1,0	3,0
	Cover and bedrock sagging	100	218,0*	1138*	1,3	3,6
Bruno *et al* (2008)						
Apulia (Italy)	–	58	–	75	4	6
Kaufmann *et al* (1999)						
Tournaisis area (Belgium)	Cover collapse	145	–	30,0	–	12,5
Hyatt *et al* (1993)						
Dougherty Plain in Albany Georgia (USA)	Bowl, undercut and shaft form	53	4,73 median = 1,84 σ = 9,24	–	μ = 0,90 median = 0,66 σ = 0,76	–
Buttrick *et al* (2008)						
South of Pretoria (South Africa)	–	640	6	–	–	–
Brinkmann *et al* (2008)						
Florida (USA)	–*	293	From 31 to 1144 183 σ = 153*	1144*	–	27

* The very large sinkholes may in fact be dolines.

Table 2 Sinkhole diameter – fitted distribution parameters

Fitted distribution details		
Distribution	**Distribution parameters**	**Kolmogorov Smirnov statistic**
Lognormal	σ = 0,72931 μ = 1,6331	0,3229

number of sources in the literature. Hyatt *et al* (1996), Bruno *et al* (2008) and Brinkmann *et al* (2008) indicated that the sizes of sinkholes follow a positively skewed lognormal distribution.

In order to establish a statistical distribution of the average sinkhole sizes that could be expected, the data pertaining to the average sinkhole diameter or length and the maximum sinkhole sizes given in Table 1 were used. It effectively translates to a sample size of 1 393 data points, comprising average and maximum sinkhole sizes only. The shaded data was excluded due to insufficient data, or since the large sinkholes sizes reported may be dolines. The software programme, EasyFit Professional Version 5.1, was used to select the numerical function that provides a good fit in respect of

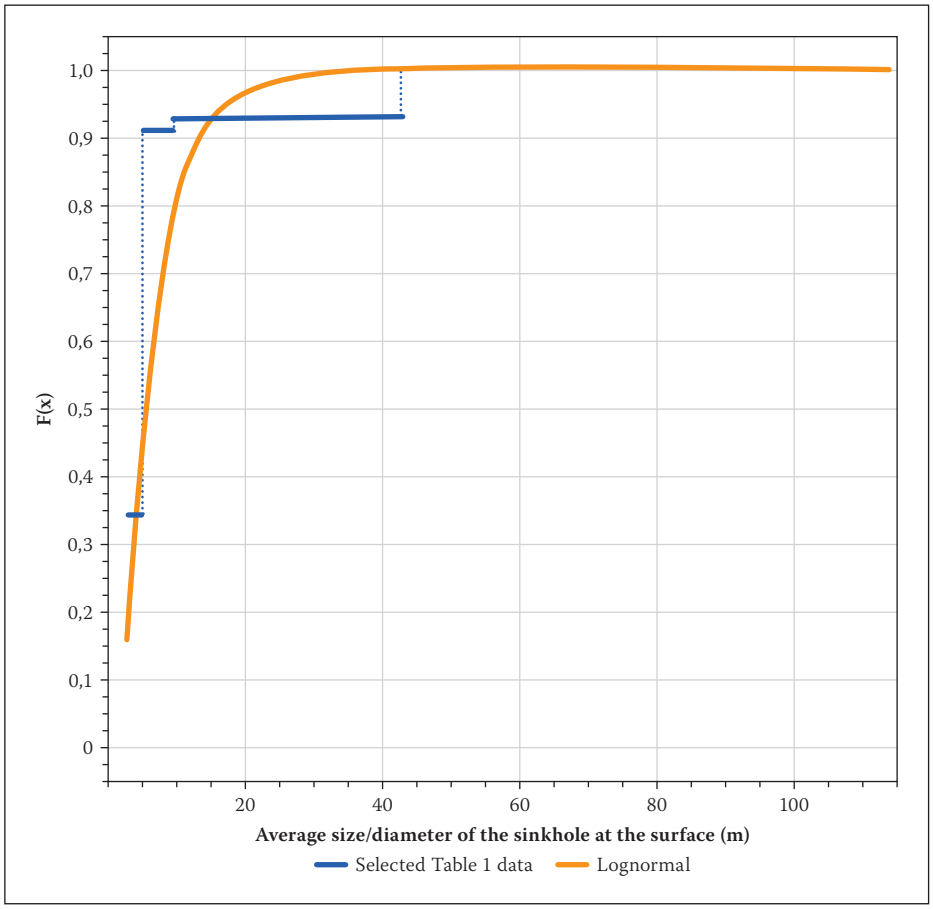

Figure 7 Sinkhole sizes – selected Table 1 data and fitted cumulative distribution function

Table 3 Dolomitic area risk characterisation framework (after Department of Public Works 2004)

Inherent risk class	Sinkhole size (diameter)			
	Small (<2 m)	Medium (2–5 m)	Large (5–15 m)	Very large (>15 m)
Inherent risk categorisation				
Class 1	Low	Low	Low	Low
Class 2	Medium	Low	Low	Low
Class 3	Medium	Medium	Low	Low
Class 4	Medium	Medium	Medium	Low
Class 5	High	Low	Low	Low
Class 6	High	High	Low	Low
Class 7	High	High	High	Low
Class 8	High	High	High	High

the average sinkhole diameter data. The Kolmogorov-Smirnov test was applied to test the goodness of fit of the data compared to a range of hypothesised distribution functions. The Kolmogorov-Smirnov statistic is based on the largest vertical difference between the theoretical and empirical cumulative distribution function. The parameters of the sinkhole size probability density function and the value of the Kolmogorov-Smirnov statistic are given in Table 2. A plot of the Table 1 data used and the fitted cumulative distribution function related to the anticipated sinkhole sizes are shown in Figure 7. The variables in the lognormal distributions are to the base e.

Although the data used comprised a limited data set, it does provide an indication of the probability that a certain sinkhole size may be exceeded. However, this distribution cannot be generally applied to all areas, due to the fact that each area is unique in relation to the factors and conditions that may determine the actual size of the sinkhole that may form. What will add great value is that data related to sinkhole sizes should be gathered in order to provide more reliable sinkhole frequency distributions for specific areas.

RISK CLASSIFICATION OF DOLOMITIC LAND

The probability of sinkhole formation exihibits great spatial variations, influenced by the stratigraphy and geological history of an area, as well as by anthropogenic processes. The risk classification of dolomitic areas entails mapping the areas where sinkholes are likely to occur, and should ideally also estimate their size and probability of occurrence.

Galve *et al* (2009) described different methods that can be applied to assess the susceptibility of dolomitic land subject to sinkhole formation, namely:

- Deterministic models (based on numerical models or stability analysis) are used to assess the degree of stability at different points. These models are based on numerical supposition, rely on data that is often difficult and expensive to obtain, does not take account of the complexity of subsidence processes and cannot be applied to large areas.
- Direct mapping of susceptibility zonations comprise maps produced by experts with a good knowledge of the study area and the phenomena, based on specific criteria used.
- Susceptibility maps based on the spatial distribution of sinkholes. A number of approaches exist:
  - Sinkhole density maps.
  - Sinkhole susceptibility zonations determined by the distance of each point in an area to the nearest sinkhole and expressing it in terms of a nearest neighbour index.
- Heuristic methods that base susceptibility assessments on the establishment of a scoring system to a group of conditioning factors.
- Probabilistic methodologies derive the probability of sinkhole formation from the analysis of statistical relationships between the known sinkholes and a group of factors used to predict sinkhole formation.

Thomas *et al* (1999) described a number of site characterisation methods which may be used to locate sinkholes or subsurface voids. It is stated that the reliability of the methods to locate existing sinkholes is generally good, but that the reliability associated with finding subsurface voids is dependent on the number of probes utilised in the area under investigation. These methods can comprise deterministic models, direct mapping of zones subject to sinkhole formation or the preparation of susceptibility maps.

Table 4 Probability of sinkhole formation (Buttrick *et al* 2001)

Inherent risk categorisation	Anticipated ground movement events (Number/km^2/yr)
Low	<=0,5
Medium	>0,5 and <=5
High	>5

A number of heuristic methods have been developed. The method of scenario supposition for the stability evaluation of dolomitic areas was developed to characterise dolomitic areas in respect of the risk of sinkhole formation (Buttrick 1992; Buttrick *et al* 2001; Department of Public Works 2004). In terms of this method, dolomitic areas are divided into eight inherent risk classes. Each inherent risk class is a function of the size of the sinkhole that may develop, as well as the anticipated number of ground movement events that may occur per unit area per year, based on the assumption that infrastructure services in dolomitic areas are poorly maintained. The framework of this method is outlined in Table 3.

Buttrick (2001) related the number of anticipated ground movement events that may occur to an area's inherent risk categorisation, as reflected in Table 4.

The above review on sinkhole probability and sizes provides a number of useful preliminary pointers. The size distribution of sinkhole sizes shown in Table 1 with its mathematical description in Figure 7 should be further reinforced with an analysis of actual sinkhole data. The risk classification framework of Buttrick (2001) provides an estimate of the probability of sinkhole formation, as well as a rough indication of which sizes can be expected. Before the analysis of sinkhole sizes causing pipeline failures can be done, the factors affecting the failure of pipelines in dolomitic areas have to be considered. Following this, one can narrow down the problem by establishing the critical sinkhole size which would pose a real danger to a welded steel pipe collapsing. This is the topic in the remainder of the paper.

FACTORS AFFECTING THE FAILURE OF PIPELINES IN DOLOMITIC AREAS

The soil angle of internal friction

The soil angle of internal friction plays an important role in determining the size and shape of the sinkhole that may form, influenced by the thickness of the blanketing layer, intrusive layers within the blanketing layer and the position of the water table.

Table 5 Soil angle of internal friction – various sources

Soil material	Soil angle of internal friction (degrees)				
	Sources of data				
	Spangler *et al* (1984)		Buttrick (1992)		Pilecki *et al* (2006)
Clays	0	10			15
Wet, fine silty sand	15	30			
Dry sand	25	40			39
Gravel	30	40			39
Loose and compact loam	30	45			
Compact clay	25	45			
Cinders	25	45			
Compact sand clay	40	50			
Silty clay (wad)			45	60	
Clayey silt (wad)			45	75	
Alternating chert and silty clay			80	90	
Chert rubble with clayey silt			45	90	
Chert and shale				90	

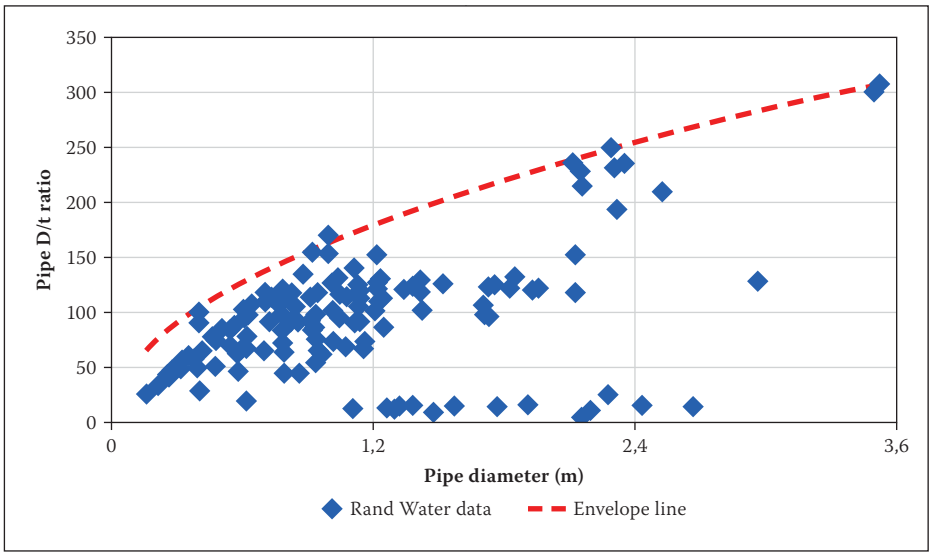

Figure 8 D/t ratio of Rand Water steel pipes installed (Reyneke 2007)

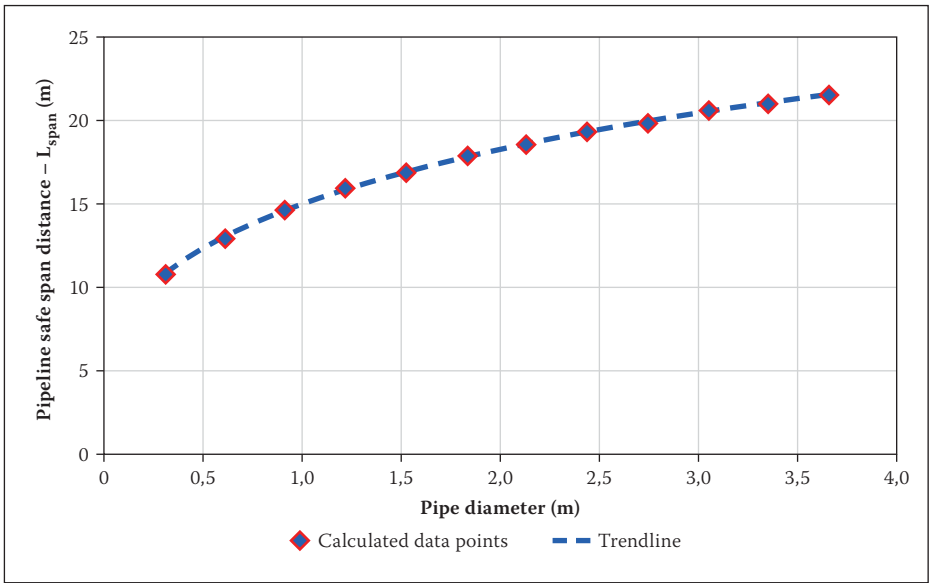

Figure 9 Pipe diameters versus pipe safe span distance relationship

Table 6 Pipeline depth of cover (Turnbull 1996)

Pipeline diameter (mm)	Minimum cover to pipeline (m)
600	0,70
1 000	0,80
1 500	0,90
2 100	1,00
2 900	1,00
3 500	1,00
4 000	1,20

Table 5 summarises the angle of internal friction of various soil types (Spangler *et al* 1984; Buttrick 1992; Pilecki *et al* 2006). The angle of internal friction of a specific soil may be further influenced by the degree of soil compaction, the soil moisture content, etc.

The pipeline depth of cover

Assuming that the geometric form of sinkholes is predominantly conical in shape (VRI = 1), it follows that the unsupported length of pipe spanning across a sinkhole will increase as the pipeline depth of cover decreases. The depth of cover over a pipeline is governed by a range of factors, such as local soil conditions, pipeline loading, water table, third party activities in the area, etc. Table 6 reflects data used by Rand Water related to the minimum depth of cover when pipelines are installed (Turnbull 1996).

An envelope line intersecting or being below the data in Table 6 is given by Equation (5).

$$h_{cover} = 0{,}8D^{0{,}21} \quad (5)$$

where

h_{cover} is the pipeline depth of cover in m

D is the diameter of the pipeline in m

The pipeline wall thickness

Bulk water distribution pipelines are designed to safely accommodate internal pressure, external loads, handling, buckling, circumferential and longitudinal deflections, and to span between supports where required. Depending on the pipeline coating or lining that will be applied, special consideration has to be given to limit the strain in the pipeline material.

Analysis of Rand Water's steel pipeline data (Reyneke 2007) indicated that pipelines are generally conservatively designed. The pipeline design stress is limited to 55% of the yield stress, while steel pipelines that have a cement mortar lining are designed so that the strain in the pipeline does not

Table 7 Pipeline safe span distance – L_{s_span} (AWWA 2003)

Pipe diameter (mm)	Wall thickness (mm)									
	4,8	6,4	7,9	9,5	11,1	12,7	15,9	19,1	22,2	25,4
	Span between supports (m) with pipe D/t ratio in brackets									
305	12,2 (64)	13,4 (48)	14,3 (38)							
610	12,8 (128)	14,6 (96)	15,8 (77)	16,8 (64)	17,7 (55)	18,3 (48)				
914	13,4 (192)	15,2 (144)	16,5 (115)	17,7 (96)	18,9 (82)	19,8 (72)	21,3 (58)			
1219		15,5 (192)	17,1 (154)	18,3 (128)	19,5 (110)	20,4 (96)	22,3 (77)	23,8 (64)		
1524		15,5 (240)	17,4 (192)	18,6 (160)	19,8 (137)	21 (120)	22,9 (96)	24,4 (80)		
1829		15,8 (288)	17,7 (230)	18,9 (192)	20,1 (165)	21,3 (144)	23,5 (115)	25 (96)	26,5 (82)	28 (72)
2134			17,7 (269)	19,2 (224)	20,4 (192)	21,6 (168)	23,8 (134)	25,3 (112)	27,1 (96)	28,7 (84)
2438			17,7 (307)	19,2 (256)	20,7 (219)	21,9 (192)	24,1 (154)	25,6 (128)	27,4 (110)	29 (96)
2743				19,5 (288)	20,7 (247)	21,9 (216)	24,4 (173)	25,9 (144)	27,7 (123)	29,3 (108)
3048					21 (274)	22,3 (240)	24,4 (192)	26,2 (160)	28 (137)	29,9 (120)
3353					21 (302)	22,3 (264)	24,7 (2110)	26,5 (176)	28,3 (151)	29,9 (132)
3658					21 (329,5)	22,6 (288.0)	24,7 (230,1)	268 (191,5)	287 (164,8)	30,2 (144,0)

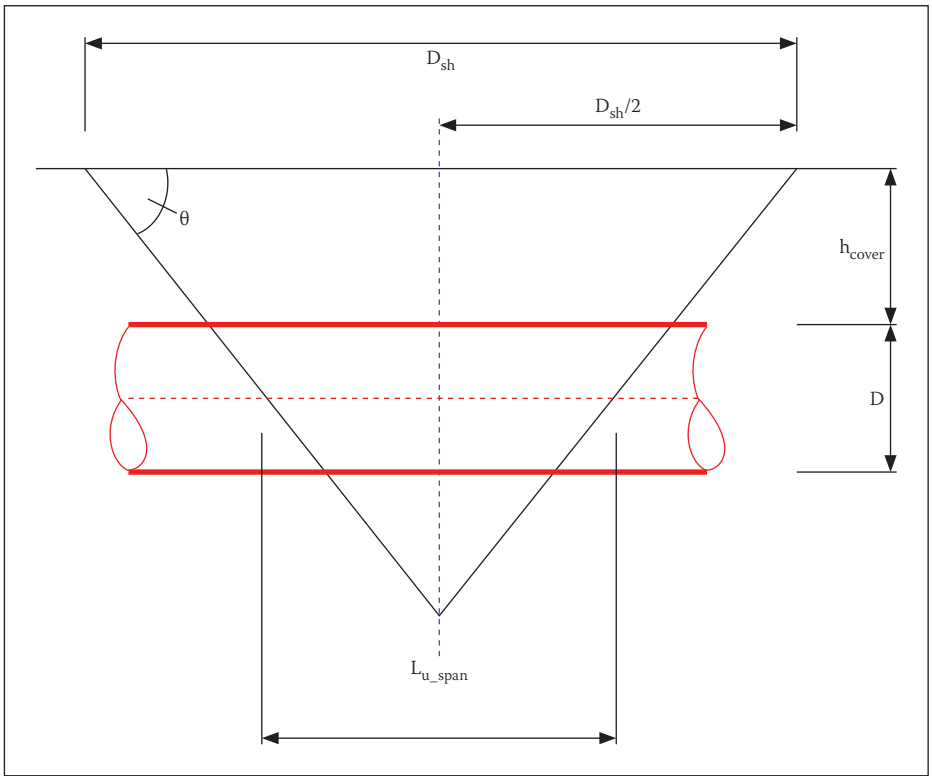

Figure 10 A pipeline intersecting a sinkhole

exceed a value of 800x10^{-6}. Figure 8 provides data pertaining to the D/t ratio versus pipe diameter relationship of Rand Water steel pipelines installed from 1907 to date.

The conservative envelope line around the data of Figure 8 is described by Equation (6).

$$\frac{D}{t} = 163 * D^{0,5} \quad (6)$$

where

D is the diameter of the pipeline in m

t is the pipe wall thickness in m

The pipeline safe span distance

AWWA (2003) provided a table that may be used to determine the safe span distances for a simply supported steel pipe, completely filled with water and supported at intervals on 120 degree contact saddles. Table 7 illustrates that a relationship exists between the pipeline safe span distance, the pipe diameter (D) and the pipe wall thickness (t). The D/t ratio has been determined for each row and column intersection, and this value is reflected together with their corresponding pipeline safe span distance (L_{s_span}) in Table 7.

Exponential interpolation between the values of Table 7, using the D/t ratio in Equation (6), allows a direct plot of the maximum safe span distance against the pipe diameter, as shown in Figure 9. A trendline was fitted to these data points and Equation (7) defines this relationship mathematically.

$$L_{s\_span} = 15D^{0,28} \quad (7)$$

where

L_{s_span} is the pipeline safe span distance

D is the diameter of the pipeline in m

SINKHOLE DIAMETERS, POSITIONS AND THE NUMBER OF EVENTS INFLUENCING THE FAILURE OF STEEL PIPELINES

Critical sinkhole diameter for a pipe running through its centre

A sinkhole that may form under specific conditions and that is large enough in diameter will leave a certain length of unsupported pipe across the sinkhole (L_{u_span}), as shown in Figure 10. The following assumptions are made related to the derivations that follow:

- A sinkhole is conical in shape, and symmetrical about its vertical axis.
- Only steel pipelines with welded joints are considered.
- The throat size of a sinkhole, which can vary greatly, is not taken into account in terms of its potential to affect the failure of the pipeline passing through the sinkhole.

Equation (8) is derived by considering the geometrical relationships within Figure 10 and expresses the diameter of the sinkhole as a function of the pipe diameter, pipeline unsupported span distance across the sinkhole, soil angle of internal friction, as well as the pipeline depth of cover.

$$D_{sh} = L_{u\_span} + \left[\frac{2 * h_{cover} + D}{\tan(\theta)}\right] \quad (8)$$

where

D_{sh} is the diameter of the sinkhole at the ground surface in m

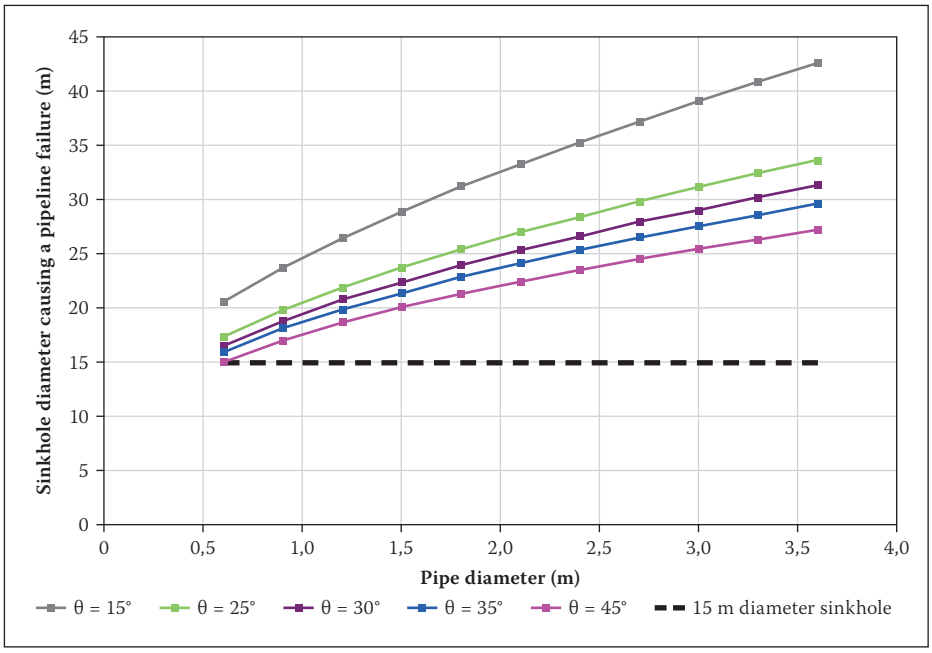

Figure 11 Minimum sinkhole diameter causing a pipe running through its centre to fail

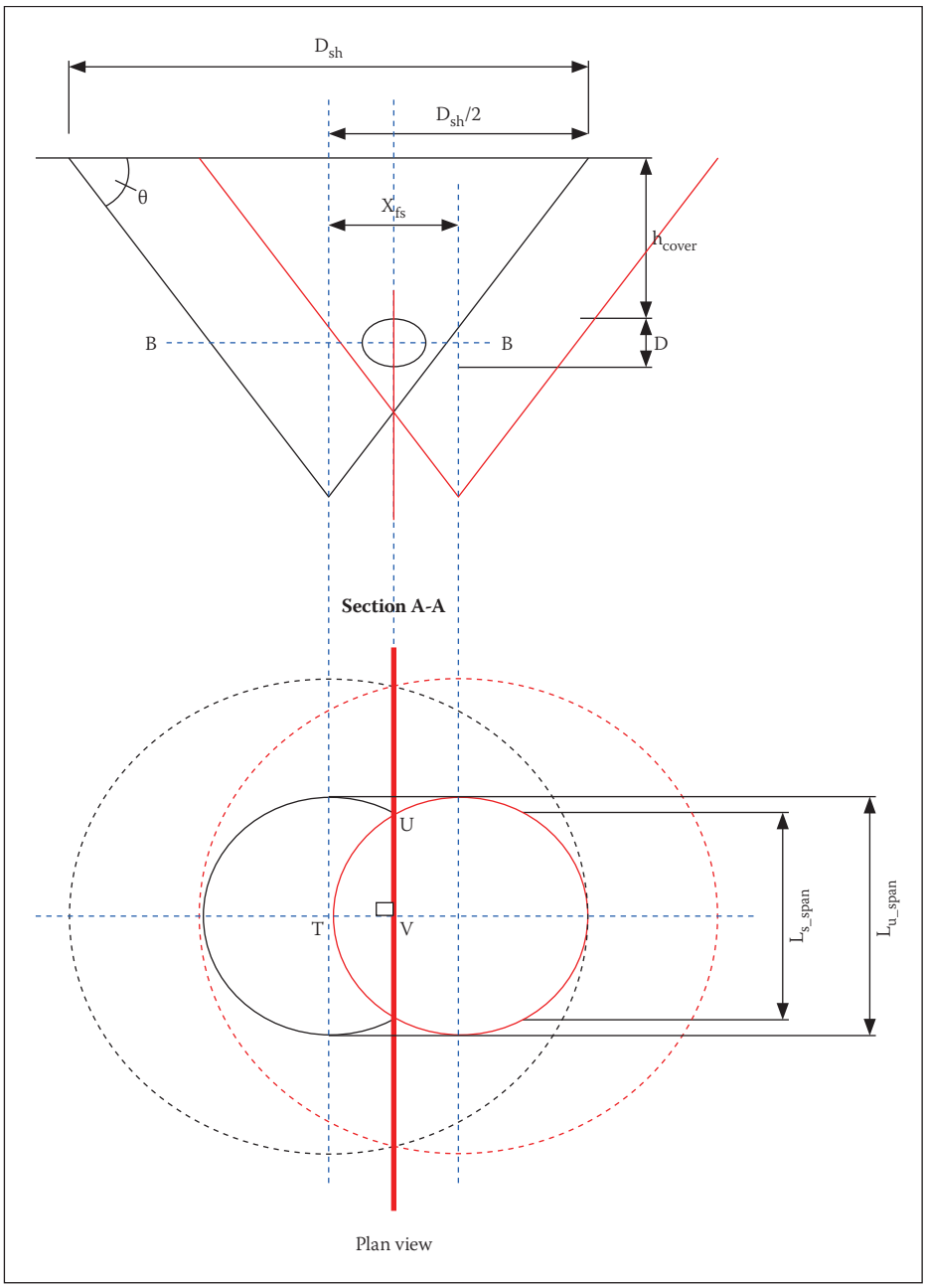

Figure 12 Sinkhole in different positions relative to the pipeline

L_{u_span} is the pipeline unsupported span distance across the cavity caused by the sinkhole in m

h_{cover} is the pipeline depth of cover in m

D is the diameter of the pipeline in m

θ is the soil angle of internal friction in degrees

Equation (9) is obtained by substituting h_{cover} from Equation (5) into Equation (8), as well as setting $L_{u\_span} = L_{s\_span}$ and substituting it into Equation (8). Equation (9) provides the maximum sinkhole diameter that can be spanned by a pipeline across its centre without structural collapse.

$$D_{sh} = 15D^{0,28} + \left[\frac{1,6D^{0,21} * h_{cover} + D}{\tan(\theta)}\right] \qquad (9)$$

Equation (9) has been applied to a range of pipeline diameters and soils with different angles of internal friction. The results thereof are shown in Figure 11, illustrating that sinkholes with a surface diameter less than 15 m pose no risk to pipelines larger than 600 mm in diameter where the soil angle of internal friction is within the range $15° \leq \theta \leq 45°$.

The zone of influence of sinkholes larger than the critical sinkhole diameter

In the previous section, it was assumed that the pipeline runs through the centre of the sinkhole. In this section, the analysis will be broadened to cases where the pipeline may intersect a sinkhole at any position. The objective is to estimate the width of the pipeline failure strip within the sinkhole, associated with sinkholes larger than the critical sinkhole diameter that will cause pipeline failure. Figure 12 depicts a sinkhole in different positions relative to the pipeline.

For the purpose of the derivation that follows, it is assumed that the sinkhole approaches and crosses the pipeline at right angles. The first critical point occurs as the sinkhole is moving towards the pipeline (from left to right) and is just in the position where the pipe reaches the limit of its unsupported span distance, L_{s_span}. As the sinkhole moves further towards the right, through a distance of $X_{fs}/2$, it will reach a point where the pipeline unsupported span distance (L_{u_span}) will be a maximum. From here, if the sinkhole moves through a further horizontal distance $X_{fs}/2$ to the right of the pipe it will again reach a point where the pipe will reach the limit of its safe unsupported span distance. Hereafter the pipe will again be able to support itself without collapse. Consider triangle TUV that lies on the horizontal plane that coincides with the centre line of the pipeline in Figure 12. It follows that:

Table 8 Minimum pipeline spacing requirements within servitudes (Turnbull 1996)

Pipeline diameter (mm)	Distance between centre lines of pipelines of equivalent or smaller diameter (mm)
600	3000
1000	3000
1500	4000
2100	5000
2900	6000
3500	7000
4000	8000

$$\left[\frac{L_{u\_span}}{2}\right]^2 = \left[\frac{X_{fs}}{2}\right]^2 + \left[\frac{L_{s\_span}}{2}\right]^2 \quad (10)$$

The unsupported span distance, L_{u_span} can be determined from Equation (8):

$$L_{u\_span} = D_{sh} - \left[\frac{2h_{cover} + D}{\tan(\theta)}\right] \quad (11)$$

Equation (12) is obtained through substitution of Equations (11) into (10), and simplifying by substituting for h_{cover} and L_{s_span} using Equations (5) and (7) respectively, and solving for X_{fs}. Equation (12) is used to calculate the width of the strip within the sinkhole where a pipe would fail.

$$X_{fs} = 2 * \sqrt{\left(\frac{D_{sh}}{2} - \frac{0{,}8D^{0{,}21} + D/2}{\tan(\theta)}\right)^2 - (7{,}5D^{0{,}28})^2} \quad (12)$$

where

X_{fs} is the width of the pipeline failure strip in the sinkhole in m

The number of sinkhole events likely to occur along a length of pipeline within a dolomitic area

Consider a pipeline of length *Ls*, traversing land where the sinkhole failure rate is λs. The number of sinkholes that are likely to occur along this length of pipeline can be calculated as follows:

$$Ns = \frac{X_{fs} * Ls * \lambda s}{1\,000\,000} \quad (13)$$

where

Ns is the number of sinkholes that may form along the section of pipeline considered per year

X_{fs} is the width of the pipeline failure strip in the sinkhole in m

Ls is the length of pipeline passing through the dolomitic area subject to sinkhole formation in m

λs is the sinkhole failure rate in the dolomitic area within which the pipeline is installed, expressed as the number of events / km^2 / year

Table 9 Sinkhole failure rates for sinkholes ≥ 15 m in diameter

Inherent risk class	Number of events for which sinkholes are greater than 15 m in diameter (Buttrick 2001)
Class 1	≤0,5
Class 2	≤0,5
Class 3	≤0,5
Class 4	≤0,5
Class 5	≤0,5
Class 6	≤0,5
Class 7	≤0,5
Class 8	>5,0

The simultaneous failure of parallel pipelines

If a sinkhole occurs, it may cause the failure of more than one pipeline, since large water distribution pipelines often run side-by-side within pipeline servitudes. The spacing of adjacent bulk water distribution pipelines laid in parallel in a servitude are governed by factors such as the availability of land, diameter of the pipeline, width of the trench, local soil conditions, and required working strips. Table 8 provides a guideline in respect of requirements to be met in terms of the spacing of pipelines to facilitate installation, repair and maintenance work to take place (Turnbull 1996).

A trendline providing a good fit to the pipeline spacing data pertaining to the minimum spacing of parallel pipelines is given by Equation (14).

$$Y_{ps} = 2{,}45e^{0{,}3D} \quad (14)$$

where

Y_{ps} is the pipeline spacing of parallel pipelines (between their centre lines) in m

D is the diameter of the pipeline in m

The number of parallel pipeline failures that may be associated with a particular sinkhole that has occurred, can be determined as follows:

$$n_{pp} = INT\left[\frac{X_{fs}}{Y_{ps}}\right] \quad (15)$$

where

n_{pp} is the number of parallel pipeline failures that may be anticipated under specific soil conditions, size of sinkhole, pipe diameter, and the spacing of parallel pipelines

PIPELINE FAILURE RATE DUE TO SINKHOLES

The work undertaken in the previous sections provides a number of important contributions to the proposed methodology, namely:

- Equation (7) provides a relationship between the pipe diameter and the pipeline safe span distance.
- Equation (8) expresses the diameter of the sinkhole as a function of the pipe diameter, pipeline unsupported span distance across the sinkhole, soil angle of internal friction, as well as the pipeline depth of cover.
- Equation (9) provides a relationship between the diameter of the pipeline, the soil angle of internal friction and the sinkhole diameter that will cause pipeline failure.
- It was shown that for steel pipelines larger than 600 mm in diameter, there is no need to consider sinkholes with diameters less than 15 m if the soil angle of internal friction is within a range $15° \le \theta \le 45°$. In such instances the middle three columns of Table 3 can be disregarded.
- Equation (12) allows the width of the strip within the sinkhole where a pipe would fail to be calculated.
- Equation (13) makes it possible to estimate the number of sinkholes, for any given sinkhole size, that could cause pipeline failure along a certain length of pipeline.
- Equation (15) makes it possible to determine the number of parallel pipeline failures that may be anticipated under specific soil conditions, size of sinkhole, pipe diameter, and the spacing of parallel pipelines

The proposed methodology

What remains is to develop a method to calculate the pipeline probability of failure that takes account of the sinkhole size and its probability of occurrence. The proposed methodology will utilise the dolomitic risk classification framework developed by Buttrick (2001) related to the relationships that exist between the eight inherent risk classes, the sinkhole sizes and the sinkhole failure rates, as reflected in Table 9. The methodology to be developed in this paper will be developed for a pipeline that falls within one inherent risk class only, while it will also only consider sinkholes greater than 15 m in diameter.

The number of sinkholes that may occur along the length of a pipeline falling totally within an inherent risk class is determined as follows:

- The base sinkhole diameter is denoted by $D_{sh(15)}$
- The sinkhole event failure rate, assuming that all sinkholes that will occur are equal to or greater than $D_{sh(15)}$, is equal to λs. The value of λs is given in Table 9.

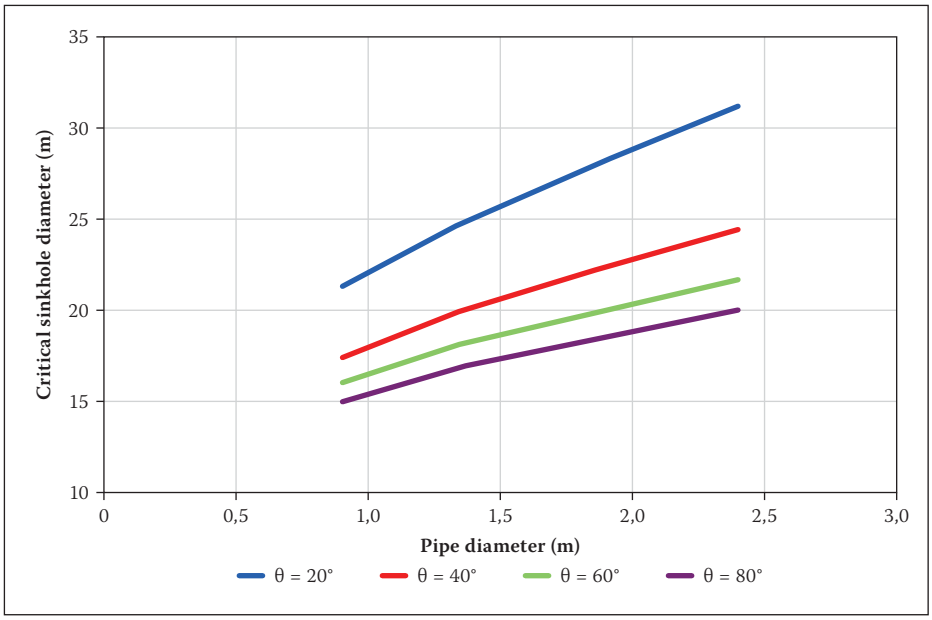

Figure 13 Critical sinkhole diameter

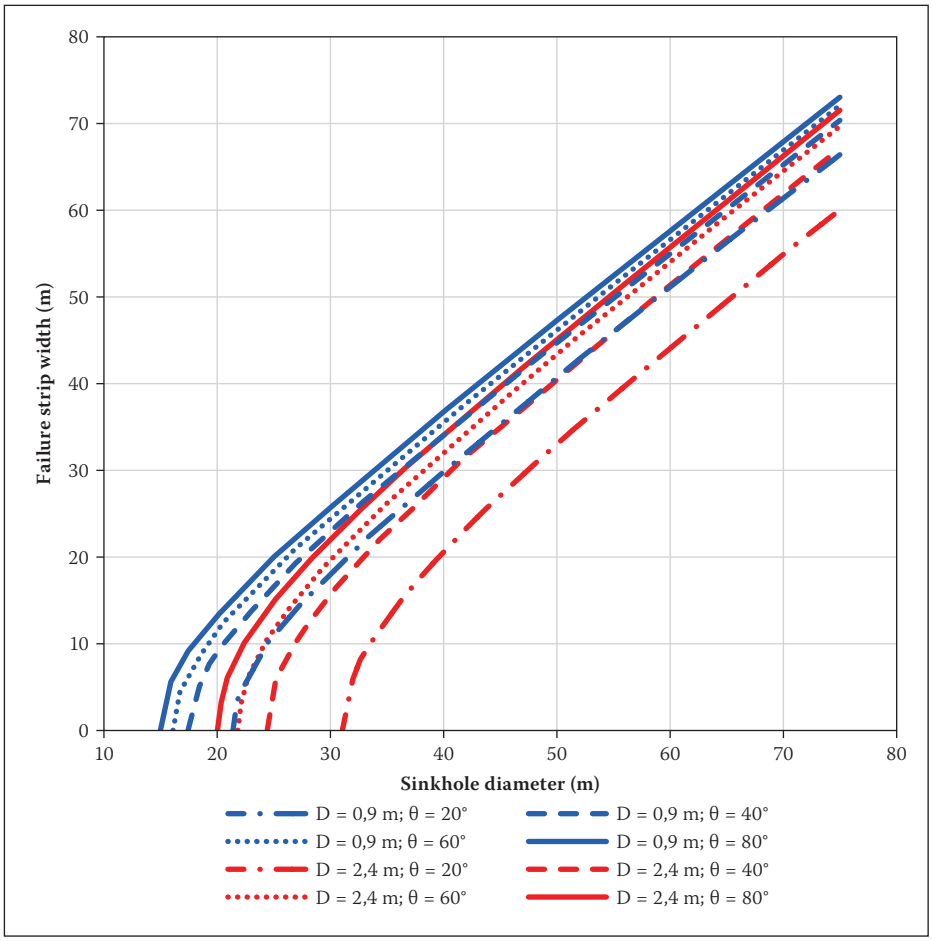

Figure 14 Pipeline failure strip width

- For sinkholes equal to or greater than D_{sh}, where D_{sh} is larger in size than $D_{sh(15)}$, the sinkhole event failure rate, λ_{Dsh}, is calculated as follows:

$$\lambda_{Dsh} = \lambda s * \frac{F(D_{sh})}{F(D_{sh(15)})} \quad (16)$$

where

λ_{Dsh} is the sinkhole event failure rate associated with sinkhole sizes equal to or greater than D_{sh} ($D_{sh} \geq D_{sh(15)}$), expressed as the number of sinkholes occurring/km^2/year

λs is the sinkhole event failure rate associated with sinkhole sizes equal to $D_{sh(15)}$, expressed as the number of sinkholes occurring/km^2/year

$F(D_{sh})$ is the probability that sinkholes equal to or greater than D_{sh} will occur

$F(D_{sh(15)})$ is the probability that sinkholes equal to or greater than 15 m will occur

$F(D_{sh})$ and $F(D_{sh(15)})$ should be based on sinkhole failure rate data in the area under investigation in order to obtain the relationship between the sinkhole size and its probability of exceedance. In this paper, the relationships will be based on the lognormal distribution function of which the parameters are provided in Table 2.

- The number of sinkholes larger than D_{sh} that may occur along the length of pipeline is determined using Equation (17).

$$Ns_{Dsh} \frac{X_{fs(Dsh)} * Ls * \lambda_{Dsh}}{1\ 000\ 000} \quad (17)$$

where

$Ns_{(Dsh)}$ is the number of sinkholes equal to or greater than Dsh associated with inherent risk class i, measured as the number of events along the length of pipeline Ls/year

$X_{fs(Dsh)}$ is the sinkhole failure strip width in m

Ls is the length of pipeline Ls in m

- The pipeline failure rate associated with sinkhole formation is calculated using Equation (18).

$$\lambda p_{Dsh} \frac{X_{fs(Dsh)} * Ls * \lambda_{Dsh}}{1\ 000} \quad (18)$$

where

λp_{Dsh} is the pipeline failure rate, measured as the number of failures/km/year

A HYPOTHETICAL EXAMPLE

A hypothetical example will be used to illustrate the application of the methodology based on the following input parameters:

1. Pipelines installed in a dolomitic area where the sinkhole failure rate associated with sinkholes greater than 15 m in diameter will be equal to 5 events/km^2/year.
2. The soil angle of internal friction may be 20°, 40°, 60° or 80° respectively.
3. The pipeline depth of cover and the spacing of parallel pipelines are defined by Equations 5 and 14 respectively.
4. The installed pipelines will consist of the following diameters: 0,9 m; 1,2 m; 1,5 m; 1,8 m; 2,1 m and 2,4 m.
5. The probability that a specific sinkhole diameter will be exceeded is governed by the data presented in Table 2.

The methodology developed will be applied to the above input parameters, exploring different scenarios, in order to determine the following:

- The critical sinkhole diameter that may cause different pipeline diameters to fail for a range of soil types.
- The width of the pipeline failure strip within the sinkhole, associated with sinkholes larger than the critical sinkhole diameter.
- The pipeline failure rate.
- The maximum number of parallel pipeline failures that may occur.

The critical sinkhole diameter causing pipeline failure

The application of Equation 9, utilising the relevant input parameters, is used to plot the graphs shown in Figure 13. Figure 13 illustrates the following:

- The critical sinkhole diameter causing pipeline failure increases as the pipe diameter increases.
- For a specific pipeline installed, the larger the soil angle of internal friction, the smaller the sinkhole causing pipeline failure.

The width of the pipeline failure strip within sinkholes larger than the critical sinkhole diameter

The application of Equation 12, utilising the relevant input parameters, is used to plot the graphs of the sinkhole diameter versus the pipeline failure strip width for D = 0,9 m and D = 2,4 m diameter respectively, as shown in Figure 14. Figure 14 illustrates the following:

- The width of the pipeline failure strip increases as the sinkhole diameter increases.
- For a specific pipe diameter and a specific sinkhole that may cause pipeline failure, the width of the pipeline failure strip increases as the soil angle of internal friction increases.
- If a specific sinkhole has formed, and for pipelines installed in an area with a similar soil angle of internal friction, the width of the failure strip increases as the pipe diameter decreases.

The pipeline failure rate

The relevant input parameters, the data obtained in respect of the pipeline failure strip width, as well as Equations 16 and 18, are utilised to determine the pipeline failure rate. The results are presented in Figure 15 for D = 0,9 m and D = 2,4 m diameter respectively. Figure 15 illustrates the following:

- For a specific pipeline installed, the pipeline failure rate increases as the sinkhole diameter increases until it reaches a local maximum value, after which it again decreases.
- For a specific pipe diameter and a specific sinkhole that may cause pipeline failure, the pipeline failure rate increases as the soil angle of internal friction increases.

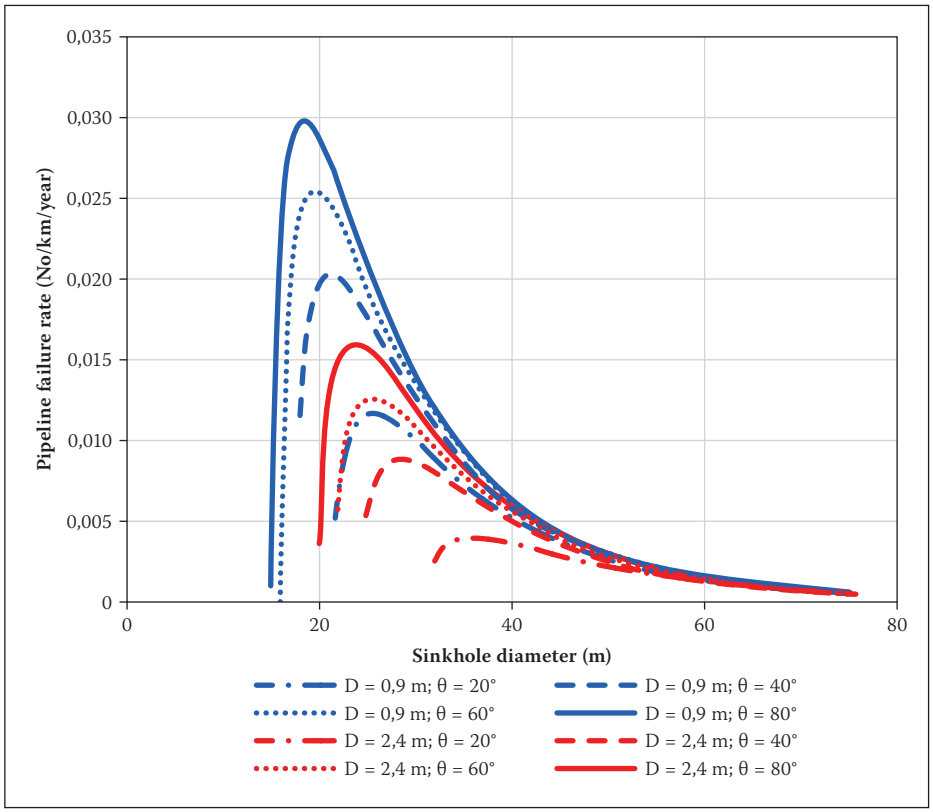

Figure 15 Pipeline failure rates – sinkholes

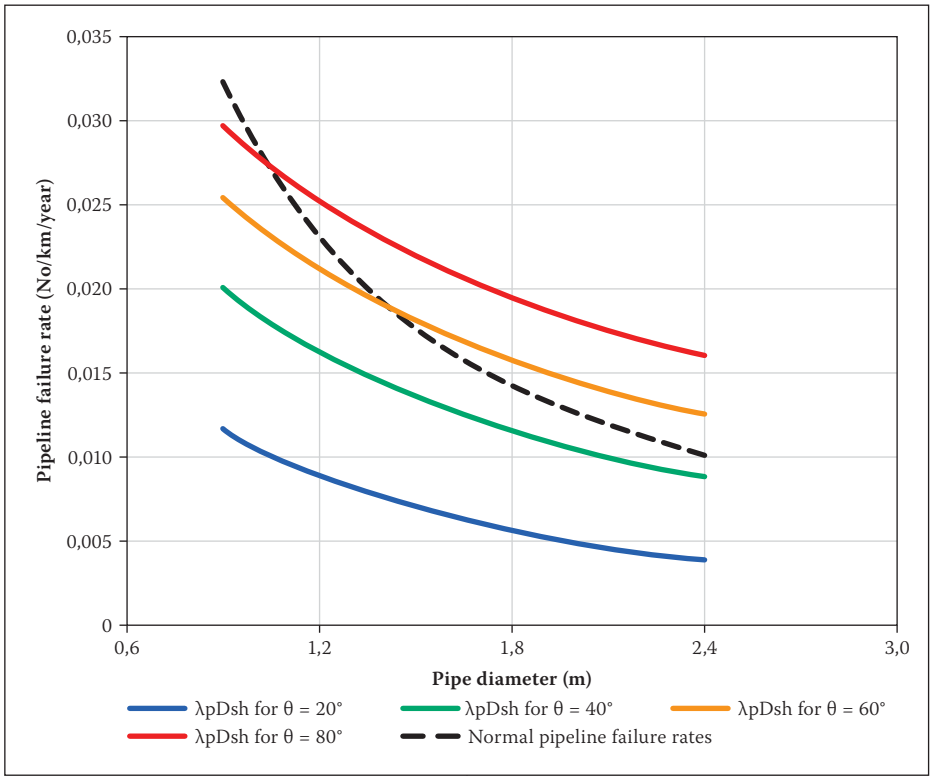

Figure 16 Maximum pipeline failure rate

- If a specific sinkhole has formed, and for a pipeline installed in an area with a similar soil angle of internal friction, the pipeline failure rate increases as the pipe diameter decreases.

For each of the curves plotted in Figure 15, it is noted that the maximum failure rate that occurs is characterised by unique values in respect of the pipe diameter, the diameter of the sinkhole that causes pipeline failure, the soil angle of internal friction and the pipeline failure rate. As a result thereof, the characteristics of all such points were determined in respect of all pipe diameter and soil angle of internal friction value combinations. The results are presented in Figures 16 and 17 respectively. The significance of these two figures relate to the fact that for a given pipe diameter installed in an area with a particular soil angle of internal friction value,

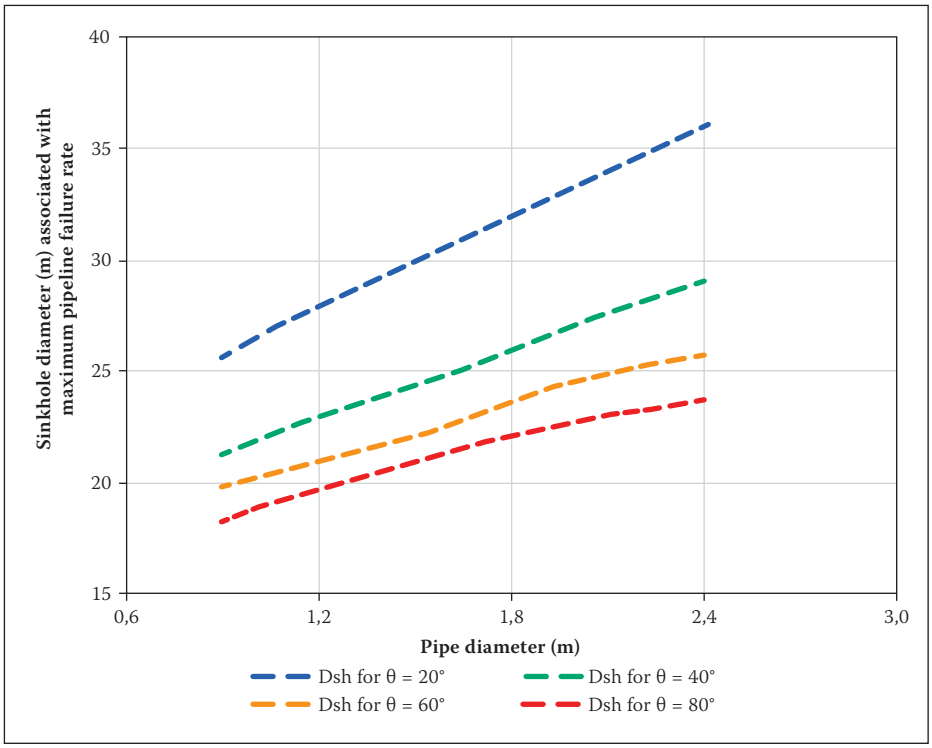

Figure 17 Sinkhole size causing maximum pipeline failure rate

Table 10 Probable simultaneous pipeline failures

Sinkhole diameter (m)	Pipeline diameter							
	D = 0,9 m				D = 2,4 m			
	Soil angle of internal friction							
	θ = 20°	θ = 40°	θ = 60°	θ = 80°	θ = 20°	θ = 40°	θ = 60°	θ = 80°
	Number of parallel pipeline failures (#)							
15				1				
16			1	2				
17		1	2	3				
18		2	3	4				
19		3	4	4				
20		3	4	5				1
21	1	4	5	5				2
22	2	4	5	5			1	2
23	3	5	5	6			2	3
24	3	5	6	6		1	2	3
25	4	6	6	7		2	3	3
26	4	6	7	7		2	3	4
27	5	6	7	7		3	4	4
28	5	7	7	8		3	4	4
29	6	7	8	8		3	4	5
30	6	8	8	9		4	4	5
31	7	8	9	9	1	4	5	5
32	7	8	9	9	2	4	5	5
33	7	9	9	10	2	5	5	6
34	8	9	10	10	3	5	5	6
35	8	9	10	10	3	5	6	6

the maximum pipeline failure rate that may occur, as well as the associated sinkhole size that will cause it, can be predicted.

A question that arises is, how critical are these pipeline failure rates when compared to normal age-related pipeline failure rates. Nel (2010) provided a relationship to calculate the pipeline failure rate for welded steel pipes, based on an analysis of published steel pipeline failure rate data, and although it was derived based on pipeline failure rate data for pipelines ≤ 800 mm in diameter. This relationship is used to determine the failure rates, and it is also plotted in Figure 16. It is noted from Figure 16 that pipeline failure rates associated with sinkholes in dolomitic areas may exceed the pipeline failure rates associated with normal pipeline failure rates, even with the sinkhole failure rate taken as low as 5 events/km^2/year. The probability of welded steel pipeline failure rates associated with sinkhole formation is therefore a significant factor that should be considered when assessing bulk water distribution reliability.

The maximum number of parallel pipeline failures that may occur within a sinkhole

The relevant input parameters, the data obtained in respect of the pipeline failure strip width, as well as Equations 12, 14 and 15 are utilised to determine the number of parallel pipeline failures that may occur within the sinkhole failure strip area. The results are presented in Table 10. Table 10 highlights the following:

- For a specific sinkhole causing pipeline failure, the number of simultaneous parallel pipeline failures decreases as the pipeline diameter increases.
- For a specific sinkhole causing pipeline failure, the number of simultaneous parallel pipeline failures increases as the soil angle of internal friction increases.

CONSIDERATION OF OTHER FACTORS THAT MAY INFLUENCE THE FAILURE OF PIPELINES IN DOLOMITIC AREAS

There are other factors that may adversely affect the failure of pipelines within dolomitic areas, such as for instance:

- The provision of services such as water pipes, sewer pipes, storm water pipes and the construction of buildings. Buttrick *et al* (2008) provided data related to the failure of pipelines attributed to dolomitic ground movement events, with reference to a study area located to the immediate south and southwest of central Pretoria (Gauteng Province, South Africa). The data presented highlighted the fact that 98,9% of the events that occurred in the study area could be attributed to leaking water services.
- Pipelines installed in areas where the pipeline may be subject to variable differential settlement along its length will experience bending stresses at the edge and centre of the depression (American Lifelines Alliance 2001). The movement of the soil around the pipeline will subject the pipeline to additional tensile and compressive stresses at the edge and the centre of the depression. The induced

stresses may cause failure of the pipeline, and high compressive stresses may cause buckling of pipelines with high D/t ratios, while tensile stresses may cause failure of the pipeline material and failure of welded joints. This may imply that a pipeline spanning an area formed by a sinkhole may fail sooner than predicted.

- Schőning (1990) and Buttrick *et al* (2008) reported that rainfall and inadequate storm water disposal tend to increase the frequency of sinkhole formation.
- The loss of water from a leaking pipeline may increase the sinkhole size and thus enhance pipeline failure.
- The support conditions at the edge of the sinkhole may be unstable due to the potential development of shear zones around the collapsed sinkhole, thus increasing the unsupported pipeline distance.
- Soil that may be present on top of the pipeline after the sinkhole has formed will increase the load carried by the unsupported pipeline and enhance pipeline failure.
- Structures that may be built around the pipeline will add an additional load to an unsupported pipeline.
- The control and channelling of scour water from pipelines will require detailed planning in dolomitic areas subject to sinkhole formation, since scour water may trigger sinkhole formation that could stimulate pipeline failure.
- The dynamic loads that may be induced onto a pipeline during sinkhole formation may also be a significant factor that should be considered.

CONCLUSIONS

The assessment of the probability of sinkhole formation and the related sinkhole diameter draws on the substantial body of experience accumulated in South Africa in the past years. Specific data and guidelines had to be adapted for the purposes of this analysis, and were complemented with a structural and spatial analysis of a steel pipe intersecting a sinkhole.

The methodology developed provides a means to predict the probability of failure of welded steel pipelines installed in areas subject to sinkhole formation. The methodology relies on the soil angle of internal friction to be known, as well as the cumulative distribution function with respect to the size of sinkholes that may be expected in an area.

The workability of the approach was demonstrated with a hypothetical example that highlighted the following aspects worth noting:

- Pipelines larger than 600 mm in diameter will most likely not fail as a result of sinkholes less than 15 m in diameter. This finding is significant since it leads to a considerable simplification of the application of the risk classification framework of Buttrick (2001).
- The maximum pipeline failure rates for pipelines between 0,9 m to 2,4 m in diameter and $20° \leq \theta \leq 80°$, are associated with sinkholes in the range 18 m to 37 m in diameter.
- Pipeline failure rates associated with sinkholes in dolomitic areas may exceed the pipeline failure rates associated with normal pipeline failure rates, even with the sinkhole failure rate taken as low as 5 events/km^2/year. The probability of welded steel pipeline failure rates associated with sinkhole formation is therefore a significant factor that should be considered when assessing bulk water distribution reliability.

The methodology developed is conservatively related to the fact that sinkholes may be more concentrated in areas where leaking wet services or ponding surface water are encountered. Furthermore, the pipeline safe span distance is based upon static forces that the pipeline is subjected to, while the dynamic forces associated with sinkhole formation are not considered. Further refinements to this methodology, as well as better and more reliable data, will undoubtedly ensure that the level of confidence related to estimating welded steel pipeline failure rates in dolomitic areas associated with sinkhole formation can be improved.

REFERENCES

American Lifelines Alliance 2001. Guidelines for the design of buried steel pipe, ASCE, 43.

AWWA (American Water Works Association) 2003. Steel pipe – A guide for design and installation. Manual of water supply practices, M11, 74.

Brink, A B A 1979. *Engineering geology of southern Africa*, Vol 1. Pretoria: Building Publications.

Brinkmann, R, Parise, M & Dye, D 2008. Sinkhole distribution in a rapidly developing urban environment: Hillsborough County, Tampa Bay area, Florida. *Engineering Geology,* 99(3–4): 169–184.

Bruno, E, Calcaterra, D & Parise, M 2008. Development and morphometry of sinkholes in coastal plains of Apulia, southern Italy. Preliminary sinkhole susceptibility assessment. *Engineering Geology,* 99: 198–209, doi:10.1016/j.enggeo.2007.11.017.

Buttrick, D B 1992. Characterisation and appropriate development of sites on dolomite, Unpublished PhD thesis, Pretoria: University of Pretoria.

Buttrick, D B, Van Schalkwyk, A, Kleywegt, R J & Watermeyer, R B 2001. Proposed method for dolomite land hazard and risk assessment in South Africa. *Journal of the South African Institution of Civil Engineering*, 43(2): 27–36.

Buttrick, D B, Watermeyer, R B, Gerber, A P, Pieterse, N & Trollip, N Y G 2008. The influence of urbanisation on sinkhole and doline formation, unpublished paper.

Department of Public Works, South Africa 2004. Appropriate development of infrastructure on dolomite. Guidelines for consultants, Report PW 344, www.info.gov.za

Galve, J P, Gutiérrez, F, Remondo, J, Lucha, P & Cendrero, A 2009. Evaluating and comparing methods of sinkhole susceptibility mapping in the Ebro Valley evaporite karst (NE Spain). *Geomorphology*, 111(3–4): 160–172, doi:10.1016/j.geomorph.2009.04.017.

Goodings, G J, Waleed, A & Abdulla, B 2002. Stability charts for predicting sinkholes in weakly cemented sand over karst limestone. *Engineering Geology,* 65: 179–184.

Hyatt, J A & Jacobs, P M 1996. Distribution and morphology of sinkholes triggered by flooding following Tropical storm Alberto at Albany, Georgia, USA. *Geomorphology,* 17: 305–316.

Kaufmann, O & Quinif, Y 1999. Cover-collapse sinkholes in the "Tournaisis" area, southern Belgium. *Engineering Geology,* 52: 15–22.

Lurie, J 1977. *South African geology for mining, metallurgical, hydrological and civil engineering.* Johannesburg: McGraw Hill.

Nel, D T 2010. *Factors that may compromise bulk water distribution reliability*. Doctoral thesis, University of Johannesburg, South Africa.

Pilecki, Z & Baranowski, A 2006. Estimation of dimension of a rectangular type sinkhole activated by abandoned shafts. Warsaw: Institute of Geophysics of the Polish Academy of Sciences, Report M-29 (395), http://agp.igf.edu.pl, 18 July 2008, 16:10.

Reyneke, P L 2007. Rand Water pipeline data. Excel spreadsheet prepared by Planning Department, Rand Water Head Office, Johannesburg.

Schőning, W L 1990.Verspreiding van sinkgate en versakkings in die dolomietgebiede suid van Pretoria. (Distribution of sinkholes and subsidence in the dolomite areas south of Pretoria). Unpublished MSc dissertation, Pretoria: University of Pretoria, pp 111–112.

Sinkhole.org 2008. Types of sinkholes. www.sinkhole.org.

Spangler, M G & Handy, R L 1984. *Soil engineering*, 4th ed. New York: Harper & Row.

Tharp, T M 1999. Mechanics of upward propagation of cover-collapse sinkholes. *Engineering Geology*, 52: 23–33.

Thomas, B & Roth, M J S 1999. Evaluation of site characterization methods for sinkholes in Pennsylvania and New Jersey. *Engineering Geology*, 52: 147–142.

Turnbull, E D 1996. A study into Rand Water's pipeline avenues and servitudes. Report of the Rand Water (South Africa) Pipelines Department, Rand water, Johannesburg.

Waltham, T, Bell, F G & Culshaw, M G 2005. *Sinkholes and subsidence. – Karst and cavernous rocks in engineering and construction*. Berlin: Springer verlag.